



Vibration-Based Method for Damage Detection at Welded Beams and Rods

Abstract

In this work, a vibration-based method for damage detection at welded beams and rods is presented. The model of the structural element includes the effect of the added inertia due to the welding process. Two methods of solution, analytically and by means of the Finite Element Method (FEM), are presented. From the results obtained it can be asseverated that the method can be a useful tool to detect degradation of welded structures. In contrast to other existing methods for cracks detection, it is shown that several frequencies have to be taken into consideration to determine the wear characteristics of the welded elements, since depending on the location of welding, some frequencies can be very little sensitive to the reduction of rigidity at the welded section. The results presented show similar tendency to those obtained by other investigations for cracks detection when added inertia was not included.

Keywords

Vibrations, welding, damage detection, non-destructive testing

P. Salgado Sánchez^a

P. López Negro^a

P. García-Fogeda^b

^a Graduate Student, ETSIAE, UPM, Madrid, Spain

^b Professor, ETSIAE, UPM, Madrid, Spain

Author email:

pablo.garciafogeda@upm.es

<http://dx.doi.org/10.1590/1679-78252881>

Received 23.02.2016

In revised form 19.06.2016

Available online 27.06.2016

1 INTRODUCTION

Welded connections may have inelastic behavior due to failure, an incorrect welding procedure or the stresses supported on their working life (Gomaa et al., (2014); Shang et al., (2003)). To verify the wear of the welded element, non-destructive testing methods (NDT) have to be applied. Among others, some methods are: visual inspection, radio-logical methods, ultrasound scanning, thermographic methods and acoustic emission (Halmshaw, (1987)). With most of them the structure has to be scanned on the precise site where the welding has been executed which sometimes might be inaccessible. As examples, one can think of large structures like bridges, oil platforms, aircraft, ship structures, etc.

Vibration-based methods (VBM) are a real alternative to classical NDT. In fact, VBM have certain advantages: the test equipment is relatively cheap, the vibration data can be collected from a

simple point or mostly on several points on the structural component, and having an access to the damaged section is not required. Therefore, a method able to measure global parameters of structures that could provide information on the structural integrity from a few selected measurement points is very attractive for non-destructive testing (Smart and Chandler, (1995); Sohn et al., (2001)).

When a welding section fails, or starts to fail, on an elastic structural element, the damage introduces local flexibility due to strain energy concentration. This effect has been already recognized and the idea of an equivalent spring has been used to quantify, in a macroscopic way, the relation between the applied load and the strain concentration around the welded section like in Adams et al. (1978).

This model has also been used for fatigue damaged structural elements, and to simulate the presence of cracks. Dimarogonas, (1996) presents a review on this problem. In the case of crack detection by VBM, different approaches have been developed. In some cases, lumped models for elastic massless elements have been used (Adams et al, (1978); Chondros and Dimarogonas, (1980); Rizos and Aspragathos, (1990); Morassi, (2000); Loya et al, (2006); Kindova-Petrova, (2014)), in others, a modified rigidity matrix has been employed in the Finite Element Method (Kisa, (2000); Saavedra et al. (1996)) and also a model of distribution of rigidity on the beam based on fracture mechanics methods has been used (Chondros et al. (1998 a)) and Chondros et al. (1998 b)); Chondros and Labeas, (2007)). In the problem of crack detection, not only the determination of the presence and size of the crack is important but also its location. Abdel-Mooty (2014) used a different approach to treat the identification of cracks based on the computation of the higher derivatives of structural modes for detecting the precise location of damage. Recently, the method has been applied for more complex systems like for crack detection on fluid-conveying pipes by Eslami et al (2016) and to solve the inverse problem of crack size and location based on the natural frequencies for an Euler-Bernoulli beam by Mostafa and Tawfik (2016). However, we are only interested in determining the quality or degradation of the welded section, showing that the added mass by the welding process has to be incorporated when modelling the system in order to reproduce the welded element behavior accurately.

The purpose of this paper is then to develop a robust and cost effective monitoring system for welded structural elements. The concept has also been applied to other welded systems like the work by Yunnus et al. (2011). After extreme events, such as earthquakes or blast loading, or due to aging and degradation resulting from operational environments, a welded section may reduce its structural properties and NDT based on vibration measurements can be a rapid condition screening to provide, in near real time, reliable information regarding the integrity of the structure. In this investigation, it is assumed that the structural element has a linear dynamic behavior before and after damage, and the detected damage is only due to the failure of the welded section. In addition, other problems due to environmental or operational conditions are assumed to not produce changes in the system response.

The model to simulate the welded section uses lumped elements. The welded is modeled as an added mass connected to the structural element by massless springs, see Figures 1 and 3 for the rod and the Euler-Bernoulli beam elements, respectively. The model allows for discontinuities in vertical displacement and rotation for the bending case, which are proportional to shear force and bending moment transmitted at the welded section as used by Loya et al. (2006) for the crack identification. The same can be applied for rotation on the torsion case.

First, in section 2.1 the model is solved analytically for both structural elements. The nonlinear characteristic equation to determine the natural frequencies of the element can have, for some values of the parameters, a slow convergence. Thus, a FEM model has also been developed in section 2.2 based on the same scheme as the analytical method. The main advantage of the FEM is the ability to treat more complex boundary conditions than the analytical solution. Both methods are compared to determine the minimum number of elements of the FEM to assure convergence. From then on, only the results of the FEM are considered in section 3.

The results presented show that the method can be applied for damage detection of welded structural elements. Attention shall be drawn to two particular points: the number of natural frequencies used for the evaluation and the added inertia during the welding process. Conclusions are presented in section 4.

2 ANALYTICAL AND FINITE ELEMENT MODEL

As mentioned, two methods have been developed to determine the dynamic characteristics of a welded rod or beam. One is based on the analytical formulation, for the treatment of ideal boundary conditions, and the other on the Finite Element Method (FEM). The first one ends up with a highly nonlinear characteristic equation that is to be solved for any value of the different parameters involved in the model definition. This can be sometimes difficult, when regular nonlinear methods may converge very slowly. Therefore, it is used as a test method to determine the number of elements to be used in the FEM model to ensure convergence for a fix set of parameters and ideal boundary conditions.

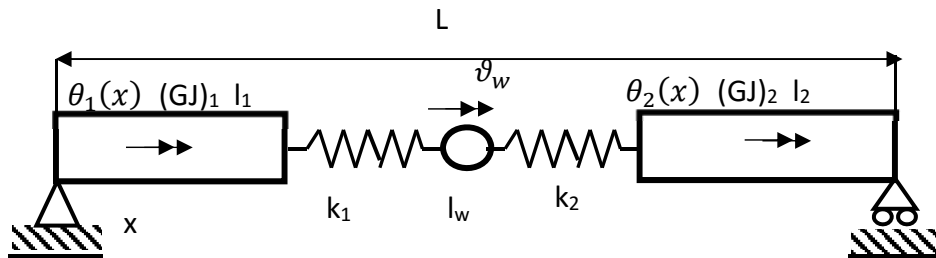


Figure 1: Model of the welding bond - torsion problem.

2.1 Analytical Model

For linear analysis, torsion and bending dynamics can be considered decoupled. Then, two elementary structures are considered in this work: a uniform rod and a uniform Euler-Bernoulli beam. The total length of the element is L and it is assumed that, at the location l_1 , the element has been repaired by a welding connection.

In the case of a rod (see Figure 1), the welding is modeled as a lumped inertia element of value I_w attached to the rod by two linear mass-less springs of rigidity k_1 and k_2 . In this way, the failure or degradation of the soldering on either side of the welded section can be investigated. The differential equations and the boundary conditions for the system are then:

$$\frac{\partial}{\partial x} \left(GJ \frac{\partial \theta_1}{\partial x} \right) - I \frac{\partial^2 \theta_1}{\partial t^2} = 0, \quad 0 \leq x \leq l_1^-; \tag{1a}$$

$$\frac{\partial}{\partial x} \left(GJ \frac{\partial \theta_2}{\partial x} \right) - I \frac{\partial^2 \theta_2}{\partial t^2} = 0, \quad l_1^+ \leq x \leq L; \tag{1b}$$

$$GJ \frac{\partial \theta_1}{\partial x} = k_1 (\vartheta_w - \theta_1) \text{ at } x = l_1^-; \tag{1c}$$

$$GJ \frac{\partial \theta_2}{\partial x} = k_2 (\theta_2 - \vartheta_w) \text{ at } x = l_1^+; \tag{1d}$$

$$I_w \vartheta_w = k_1 (\vartheta_w - \theta_1) - k_2 (\theta_2 - \vartheta_w); \tag{1e}$$

where ϑ_w is the generalized coordinate which determines the rotation of the lumped inertia term due to the welded material, θ_1 and θ_2 are the dynamic deformation of the rod at $0 \leq x \leq l_1^-$ and $l_1^+ \leq x \leq L$, respectively, GJ the torsion rigidity of the rod, and I the polar moment of inertia per unit length of the rod.

Equations (1a) to (1e) should be completed with the ideal boundary conditions at the rod ends. For the case of simple supported end conditions ($\theta_1(0) = 0$ and $\theta_2(L) = 0$), equations (1a) to (1e) can be solved to obtain the characteristic equation:

$$\left(\frac{\delta_1}{1 + \lambda} \right)^2 \left[X \cos(X\lambda) + \frac{\delta_2}{1 + \lambda} \sin(X\lambda) \right] \sin X + \left(\frac{\delta_2}{1 + \lambda} \right)^2 \left[X \cos X + \frac{\delta_1}{1 + \lambda} \sin X \right] \sin(X\lambda) + \left[-s(1 + \lambda)X^2 + \frac{\delta_1 + \delta_2}{1 + \lambda} \right] \left[X \cos X + \frac{\delta_1}{1 + \lambda} \sin X \right] \left[X \cos(X\lambda) + \frac{\delta_2}{1 + \lambda} \sin(X\lambda) \right] = 0, \tag{2}$$

where the different parameters are:

$$X = \beta l_1, \quad \lambda = \frac{L}{l_1} - 1, \quad s = \frac{I_w}{IL}, \quad \delta_1 = \frac{k_1 L}{GJ}, \quad \delta_2 = \frac{k_2 L}{GJ} \text{ and } \beta^2 = \frac{\omega^2 I}{GJ}.$$

The roots of equation (2) can be obtained numerically for the unknown frequency parameter β (solving X) as a function of the different parameters of the problem. However, this equation results to be too stiff so convergence may be sometimes tedious since the range of the parameters, like δ_1 , can be very extent. Therefore, as it will be presented at section 2.2, a finite element procedure based on the same model presented in Figure 1 has been developed. We remark that the main advantage of the FEM model is that other end boundary conditions can be considered such as non-ideal boundary conditions introducing flexible supports as sketched in Figure 2.

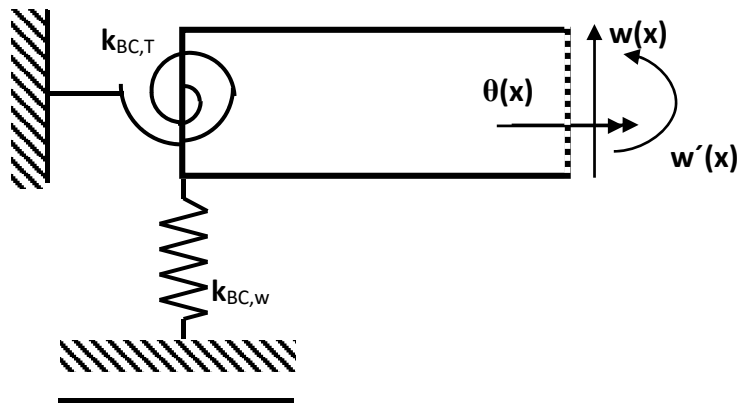


Figure 2: Non-ideal boundary conditions.

To guaranty the convergence of the FEM model for specific values of the parameters, the results for the first four natural frequencies have been calculated as function of the number of elements N_{FE} and compared with the results of the analytical solution. In this way, the analytical solution is used to validate the FEM model in both cases.

For the case of an Euler-Bernoulli beam in bending vibration, the model considered is illustrated in Figure 3. The mass added by the welding process is represented by a lumped mass of value m_w and a rotational moment of inertia I_w . This mass is attached to both sides of the beam by two linear translational springs of value k_1 and k_2 , and two linear rotational springs of values k_{T1} and k_{T2} , all of them with zero inertia. The linear translational (torsion) springs oppose to vertical displacements (rotation) between both sides of the beam.

For the uniform beam considered, the formulation of the vibration problem can be expressed as:

$$\frac{\partial^2}{\partial x^2} \left(EI \frac{\partial^2 w_1}{\partial x^2} \right) + m \frac{\partial^2 w_1}{\partial t^2} = 0, \quad 0 \leq x \leq l_1^-; \tag{3a}$$

$$\frac{\partial^2}{\partial x^2} \left(EI \frac{\partial^2 w_2}{\partial x^2} \right) + m \frac{\partial^2 w_2}{\partial t^2} = 0, \quad l_1^+ \leq x \leq L; \tag{3b}$$

$$m_w z_w + k_1 (z_w - w_1) + k_2 (z_w - w_2) = 0; \tag{3c}$$

$$I_w \theta_w + k_{T1} \left(\theta_w - \frac{\partial w_1}{\partial x} \right) + k_{T2} \left(\theta_w - \frac{\partial w_2}{\partial x} \right) = 0; \tag{3d}$$

and the conditions at $x = l_1$ are given by Equations (4a) to (4d).

$$-EI \frac{\partial^2 w_1}{\partial x^2} + k_{T1} \left(\theta_w - \frac{\partial w_1}{\partial x} \right) = 0 \quad \text{at } x = l_1^-, \tag{4a}$$

$$\frac{\partial}{\partial x} \left(EI \frac{\partial w_1}{\partial x^2} \right) + k_1 (z_w - w_1) = 0 \text{ at } x = l_1^-, \tag{4b}$$

$$-EI \frac{\partial^2 w_2}{\partial x^2} + k_{T2} \left(\theta_w - \frac{\partial w_2}{\partial x} \right) = 0 \text{ at } x = l_1^+, \tag{4c}$$

$$\frac{\partial}{\partial x} \left(EI \frac{\partial w_2}{\partial x^2} \right) + k_2 (z_w - w_2) = 0 \text{ at } x = l_1^+, \tag{4d}$$

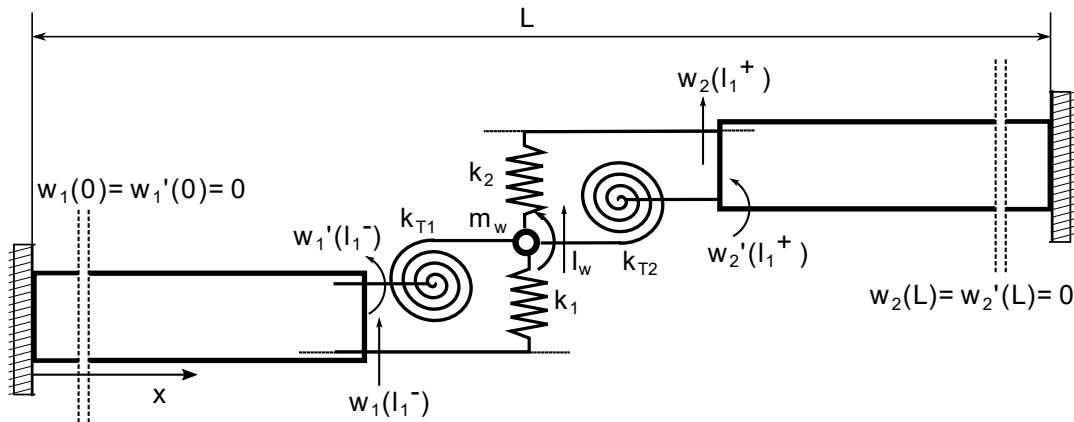


Figure 3: Model of the welding bond - bending problem.

where z_w and θ_w are the generalized coordinates which determine the translation and rotation of the lumped inertia term due to the welded material, w_1 and w_2 are the dynamic deformation of the beam at $0 \leq x \leq l_1^-$ and at $l_1^+ \leq x \leq L$, respectively; EI the flexural rigidity of the beam and m the mass per unit length of the beam.

These equations have to be completed with the boundary conditions at both ends of the beam. In the case of a clamped beam at both ends, the characteristic equation to determine the natural frequencies can be obtained by expansion of a determinant of order 6 (two of the constants of integration can be eliminated from the boundary conditions) that depends on the following parameters:

$$\lambda = \frac{L}{l_1} - 1, \quad s = \frac{m_w}{mL}, \quad \delta_1 = \frac{k_1 L^3}{EI}, \quad \delta_2 = \frac{k_2 L^3}{EI}, \quad r_\theta = \frac{I_w}{mL^3},$$

$$\delta_{T1} = \frac{k_{T1} L}{EI}, \quad \delta_{T2} = \frac{k_{T2} L}{EI} \quad \text{and} \quad \beta^4 = \frac{\omega^2 m}{EI}.$$

Like in the previous case of the torsional rod, the resulting characteristic equation can be solved numerically to determine the natural frequencies of the system from the roots of the frequency parameter. However, for this case the numerical solution is even more cumbersome than for the rod vibration element. Therefore again, the above formulation is only used as a measure of the convergence with the number of elements of the developed FEM model, based on the system of Figure 3. Again,

negligible. Therefore, it is concluded that -with this number of elements- the results of the FEM model are accurate enough.

	ω_1	ω_2	ω_3	ω_4
$s = 0.001, \delta_1 = \delta_2 = 100$				
Analytic solution	3.1260	6.2212	9.3778	12.442
FEM $N_{FE}=10$	3.1260	6.2522	9.4834	12.692
FEM $N_{FE}=100$	3.1260	6.2212	9.3790	12.445
FEM $N_{FE}=300$	3.1260	6.2212	9.3784	12.443
$s = 0.001, \delta_1 = \delta_2 = 10^4$				
Analytic solution	3.1260	6.2828	9.3784	12.5658
FEM $N_{FE}=10$	3.1260	6.3148	9.4836	12.8222
FEM $N_{FE}=100$	3.1260	6.2830	9.3792	12.5678
FEM $N_{FE}=300$	3.1260	6.2828	9.3784	12.5658

Table 1: Convergence of the torsion problem FEM model given masses (s) and stiffness's ($\delta_1 = \delta_2$) of the welded bond.

In Table 2 the first four non-dimensional natural frequencies for a beam clamped at both ends are presented as function of the number of elements. The values of the parameters are $\lambda = 1, s = 0.001, r_\theta = 0.0001$ and different sets of the translational and torsional rigidities. The results of the characteristic equation are also given for comparison. Now, it can be observed that the number of elements to achieve a negligible difference has to be between 10 and 100. From now on, the number of elements used for the analysis of this structure will be $N_{FE} = 100$. The rigidity at both sides of the lumped mass was kept for this validation case equal, i.e., $\delta_1 = \delta_2$ and $\delta_{T1} = \delta_{T2}$.

	ω_1	ω_2	ω_3	ω_4	ω_1	ω_2	ω_3	ω_4
Free beams: $[\delta_1 = 10^{-6}, \delta_{T1} = 10^{-6}]$					Rigid bond: $[\delta_1 = 10^6, \delta_{T1} = 10^2]$			
Analytic solution	0.0142	0.1414	14.349	14.349	22.373	61.671	119.68	199.83
FEM $N_{FE}=10$	0.0142	0.1276	14.350	14.350	22.216	62.498	119.74	199.48
FEM $N_{FE}=100$	0.0140	0.1415	14.350	14.350	22.212	62.497	119.73	199.44
FEM $N_{FE}=300$	0.0091	0.0906	14.350	14.350	22.212	62.497	119.73	199.44
Damaged bond: $[\delta_1 = 10^4, \delta_{T1} = 1]$					$[\delta_1 = 10^2, \delta_{T1} = 0.01]$			
Analytic solution	15.768	64.016	91.930	141.37	14.086	14.142	30.335	87.310
FEM $N_{FE}=10$	15.774	61.693	91.935	137.52	14.087	14.127	30.338	87.315
FEM $N_{FE}=100$	15.774	61.692	91.930	137.52	14.087	14.128	30.338	87.312
FEM $N_{FE}=300$	15.774	61.690	91.929	137.52	14.087	14.127	30.338	87.312

Table 2: Convergence of the bending problem FEM model for a given mass ($s = 0.01, r_\theta = 0.0001$) and various parameters of stiffness of the welded bond.

From then on, only the results of the FEM model for different values of the parameters are evaluated.

3 RESULTS AND DISCUSSION

Next, based on the FEM results, a study of the influence of the different parameters on the natural frequencies of the two problems considered -the welded rod and beam structural element- will be presented. The objective is to determine how a degraded welded joint can influence on the natural frequencies of the system. Thus, by means of a vibration test, be able to estimate the degradation of the element.

3.1 Rod Structural Element: Torsional Vibrations

The parameters considered for the torsion vibrating rod are the mass parameter s , the position of the welded section λ , the non-dimensional left-side spring rigidity δ_1 , and the non-dimensional right-side spring rigidity δ_2 , as defined in section 2.1. The initial values of all the parameters are such that the rod natural frequencies when welded are similar to those of the rod before damaged. Certainly, it could happen that the welded structural element has better dynamic properties (more rigidity) than the undamaged rod. This case, however, will not be considered in this paper.

The parameters can be estimated as follows:

$$s \sim \frac{IL_s}{IL} \sim \frac{L_s}{L}, \quad \delta \sim \frac{GJ / (IL_s)}{GJ / (IL)} \sim \frac{L}{L_s}.$$

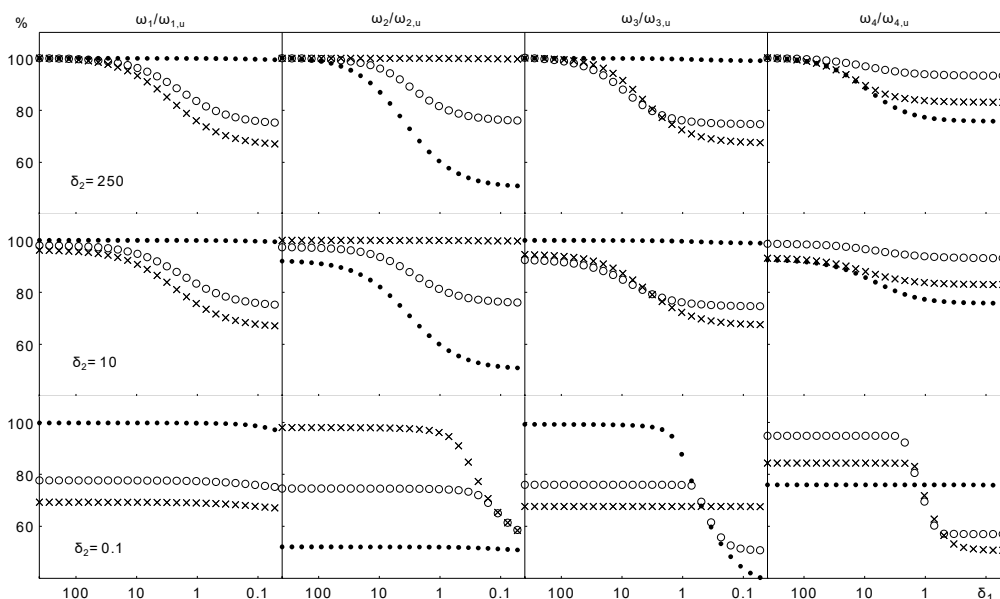


Figure 4: Evolution of the first four natural frequencies ω_i (percentage respect to the frequencies of the undamaged rod, $\omega_{i,u}$), for $\lambda = 1$ (solid), $\lambda = 2$ (circles) and $\lambda = 3$ (cross), with the variation of δ_1

and three fixed values of δ_2 . A value of $\delta_2 = 250$, $\delta_2 = 10$ and $\delta_2 = 0.001$ represents,

respectively, a rigid, a damaged and a broken bond.

In the first part of the study the mass parameter is kept to a constant value of $s = 0.01$ (the welding is performed using a material with a similar density to the rod and its length is about a 1% of the rod's length), meaning that the amount of welded material remains the same with respect to the mass of the rod. The influence of the change of this parameter will be taken into consideration afterwards.

In Figure 4, the degradation of only one side of the welding -via reducing only one non-dimensional stiffness- is investigated, while keeping the other side stiffness constant. The plots show the evolution of the first four natural frequencies with the degradation of the left-side spring δ_1 for different values of the stiffness of the right-side spring. Note that, as expected, the variation of the natural frequencies is bigger when both sides of the welding are affected.

From this figure the following conclusions can be obtained. For $\lambda = 1$, welded at the center of the rod, the odd frequencies are barely affected by the degradation. Thus, methods for crack detection based on the evolution of the first natural frequency may be unreliable for these cases. Higher order frequencies are more sensitive to rigidity losses than lower order, thus while the second frequency almost remains unchanged for $\lambda = 1$ and $\delta_2 = 250$ in the range of δ_1 between [250-50], the fourth frequency has a constant value in the reduced range of [250-100], concluding then that if the vibration method is used to determine the damage of a structural element several frequencies should be taken into consideration.

For $\lambda = 2$, the odd frequencies are more affected by the rigidity variation. When the order of the frequency is increased the range of rigidity at which the frequency remains constant is also reduced. Thus, $\omega_1 / \omega_{1,u} \sim 1$ for $\delta_1 \in [250 - 50]$ and $\omega_4 / \omega_{4,u}$ for $\delta_1 \in [250 - 100]$, although the change is less significant. For example, for $\delta_1 = 1$, $\omega_1 / \omega_{1,u} = 0.8$ and $\omega_4 / \omega_{4,u} = 0.9$. Then, it can be concluded that higher order frequencies are more sensitive to damage of the welded rod but lower order frequencies show biggest decrease when welding fails.

From the results shown in Figure 4, also the dynamic characteristics of the system as function of the different values of the parameters can be described. Thus, when the rigidity of the welded element is very small, the system behaves like two independent rod elements with a frequency close to the smaller frequency of a rod simply supported at one end and free at the other. This behavior is represented -in a schematic way- as a function of the parameter λ for the first modes in Figure 5.

The frequency parameter ν , defined as $\nu = \omega \sqrt{(IL) / (GJ)}$, is used. For the undamaged rod it is named as $\nu_{i,u}$ and for the damaged rod $\nu_{i,j}^{s,l}$. The first subscript means the mode order, the second the value of the parameter λ and the superscript refers to the shorter 's' or larger 'l' uniform rod element for the damaged rod when $\lambda \neq 1$. When the rod is undamaged the frequency parameter has the values $\pi, 2\pi, 3\pi, \dots$. If the rod is welded at the middle point $\lambda = 1$ and the section is broken, both parts of the rod have the same frequencies and the values are $\pi, 3\pi, 5\pi, \dots$ so the first two frequency parameters of the undamaged rod π and 2π collapse to a single frequency parameter of the broken rod π , the third and fourth frequency parameters collapse to the second frequency parameter of the broken rod 3π , and so on.

If the rod is welded at $\lambda = 2$ (welding section at 1/3 of the total length) and the welding is totally broken then, two sets of frequencies parameters are obtained one for each element. For the shorter

one, the frequency parameter $\nu_{i,2}^s$ has the values $3\pi/2, 9\pi/2, 15\pi/2$ for the first three frequencies and for the larger part $\nu_{i,2}^l$ the values $3\pi/4, 9\pi/4, 15\pi/4$. Now, the undamaged frequencies move in the following way, $\nu_{1,u}$ moves from π to $3\pi/4$, $\nu_{2,u}$ from 2π to $3\pi/2$, and $\nu_{3,4}$ from 3π to $9\pi/4$, and so on.

Similar reasoning can be made to explain the evolution of the natural frequencies for the other locations of the welding, for example $\lambda = 3$. In this way, it can be concluded that when one of the torsional rigidities is negligible and the other is such that the system prefers vibrating like two independent elements, the mode selected by the structure is the nearest one with smaller frequency of the cantilevered rod. Note that the relation between the frequencies ν of the undamaged rod and the broken one (cantilevered) matches with the plots given in Figure 4.

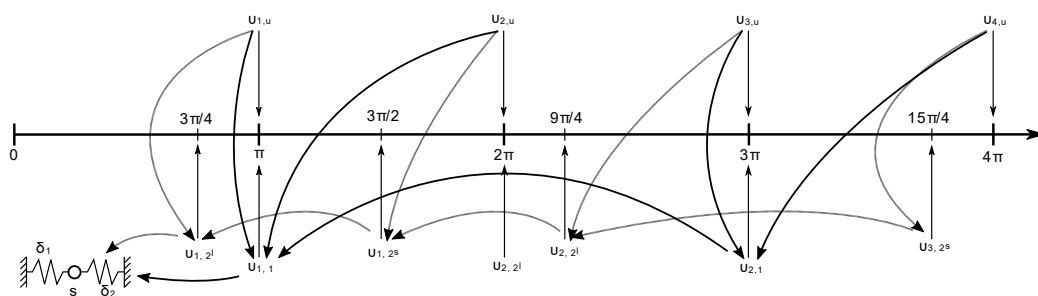


Figure 5: First non-dimensional frequencies of the rod in different conditions: with no damage on the welding $\nu_{i,u}$ and without being welded $\nu_{i,j}$. First subindex “i” denotes the i-th mode of vibration (i.e., 1, 2, 3...), the second denotes the values of the parameter λ , and the letter ‘s’ or ‘l’ if the side under consideration is the shorter or the larger one when $\lambda \neq 1$, respectively. Finally, the different curved arrows are related to the value of λ considered: 1 (thick) and 2 (thin).

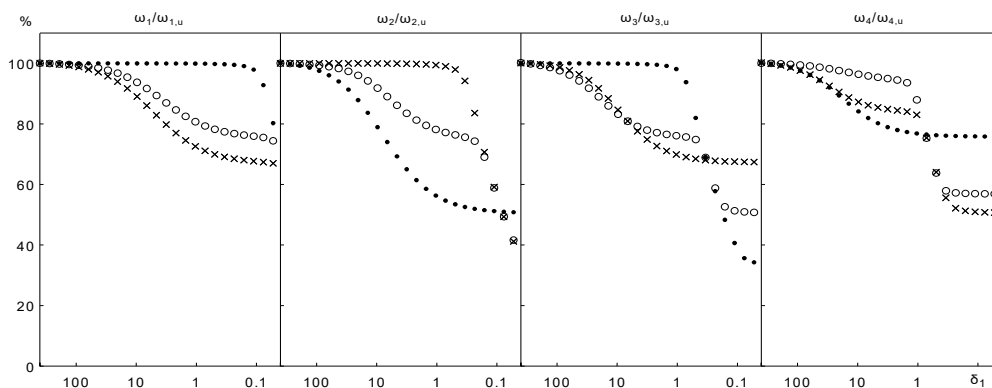


Figure 6: Evolution of the first four natural frequencies ω_i (percentage respect to the frequencies of the undamaged rod, $\omega_{i,u}$), for $\lambda = 1$ (solid), $\lambda = 2$ (circles) and $\lambda = 3$ (cross), with the variation of δ_1 (both springs have the same rigidity, $\delta_1 = \delta_2$).

Now, in Figure 6 the general damage of the welding is considered. For $\delta_1 = \delta_2$, both sides of the welding with equal rigidity, the first four natural frequencies divided by the natural frequency of the undamaged rod are presented as function of the parameter δ_1 for $\lambda = 1, 2, 3$ (welded section at 50%, 33% and 25% of the total length, respectively). In the figure it can be observed that the analysis of several frequencies has to be used to detect the damage of the welded section. When the welding is close to a node, there is a large concentration of stresses at the point and therefore the dynamic response is more sensitive to small changes in rigidity. This can be observed in the second and fourth frequencies for $\lambda = 1$, and in the third frequency for $\lambda = 3$. When damage on the welding is investigated, one is interested in detecting this damage as early as possible and, as Figure 6 suggests, the higher order of the frequency the more sensitive to decrease on rigidity. However, on real structures higher order frequencies can also be influenced by other parameters i.e., aging of the structure. Therefore, a careful analysis of all the frequencies should be made to asseverate the quality of the welding.

In addition, note that there is a critical value of δ_1 and δ_2 where the system prefers to respond as a single vibrating lumped mass when the smaller frequency of the cantilevered rod coincides with $\sqrt{(\delta_1 + \delta_2) / s}$, written in non-dimensional parameters.

In this way, one can see that starting with high values of δ_1 and δ_2 the behavior of the model will be similar as the clamped-clamped rod (undamaged). Decreasing the stiffness of the rod will lead to a change of the natural frequencies, which will tend to the corresponding frequencies of the clamped-free (cantilever) rods, as shown in Figure 5. Moreover, when the smaller frequency of the cantilever rods (corresponding to the longer structural element) is greater than $\sqrt{(\delta_1 + \delta_2) / s}$ lower frequencies will be found, but these frequencies will be associated to the motion of the lumped mass. This behavior can be observed in Figure 6 when both sides are really damaged. These values of δ_i demonstrate the model's consistency.

This result is very interesting, as it opens a further study: while at least one of the two sides of the bonds remains undamaged the lumped mass will vibrate attached to one of the structural element. If a frequency close to that of the cantilever rod is found, then one can asseverate that at least one of the two sides of the welding is highly damaged and the bond is very close to failure.

For damage detection the most important parameter is the change in frequency, independently to the damage occurring at one or both sides of the welding connection. When welding fails the natural frequencies of the system are those of the cantilever rod (slightly modified by the influence of the attached lumped mass). Therefore, no further results will be presented varying independently the two sides of the welding connection.

Next, the influence of the welding mass on the dynamic characteristics of the rod will be investigated. The mass parameter has been changed from a 0.1% of the total mass of the rod to a 1.5%. These values can be considered to cover the full possibilities of a welding connection. In Table 3, for two different values of the welding location, the influence of the added mass parameter s is presented. On the table, the values of the nondimensional rigidities δ_i to keep the natural frequency parameter equal to the values of the undamaged rod are given. Note that the increase of the welding mass (with no variation of the welding length) yields to smaller values of the natural frequencies for a fixed value of the welding rigidities. For example, to recover the first natural frequency with $\lambda = 2$ and

$s = 0.0125$, the rigidities should be modified up to a value of 725. So, a 25% increase from the value $s = 0.01$ in the welding mass leads to a 382% increase in both rigidities. Even more, there is a critical mass value when no rigidity is enough to recover the natural frequency of the undamaged rod.

λ	s	δ_1			
		v_1	v_2	v_3	v_4
2	0.0010	53	55	196	48
	0.0050	78	81	196	72
	0.0100	190	192	196	180
	0.0125	725	600	196	690
	0.0150	-	-	196	-
3	0.0010	103	0.023	107	193
	0.0050	130	0.23	134	193
	0.0100	196	18	193	193
	0.0125	265	-	246	193
	0.0150	400	-	340	193

Table 3: Value of the nondimensional rigidity δ_1 to recover the i-th frequency of the first four natural modes with the variation of the nondimensional welding mass. It was taken $\delta_1 = \delta_2$.

Some interesting cases can be observed in the table. For $\lambda = 2$, in the mass interval of interest, no stiffness changes are needed to keep constant the frequency of the third mode. This effect can be explained in terms of the eigenmodes. The third mode presents a node where the welding is placed, so there is no displacement during the vibrations in this section and therefore, the mass does not affect. The same reasoning could be applied to the fourth frequency with $\lambda = 3$. In addition, the effect of the strains/stresses concentration could be considered (via the derivative of the rotation). For $\lambda = 3$, the second frequency seems to be, for small values of s , less affected than the others and negligible rigidities are needed. In this case, the welding is placed in a zero-strain section (maximum displacement) so the relative rotation of the mass respect to the nearer regions is negligible, therefore small values of rigidity are needed to keep the mass attached when it is small. In opposition, if the mass increases, this location yields to a bigger effect and then the critical mass value commented before appears more rapidly. Thus, in a vibration test to qualify the grade of a welded structure the added mass can mislead to a wrong result. If the mass is too large, the decrease of the natural frequencies can be due to the mass effect and not to a loss of rigidity. The added mass has never been included in previous models used to study this problem. In contrast to the crack case, which treats a similar problem with no lumped mass included, we demonstrate that the present model is justified since it yields to different frequency values depending on the damage distribution on each side. A deeper study on how the mass affects the welding performances should be done with experimental results in subsequent investigations. However, this is beyond the scope of this paper and will be undertaken elsewhere.

3.2 Beam Structural Element: Bending Vibrations

Next, the dynamic characteristics of an Euler-Bernoulli beam element are investigated as function of the different parameters.

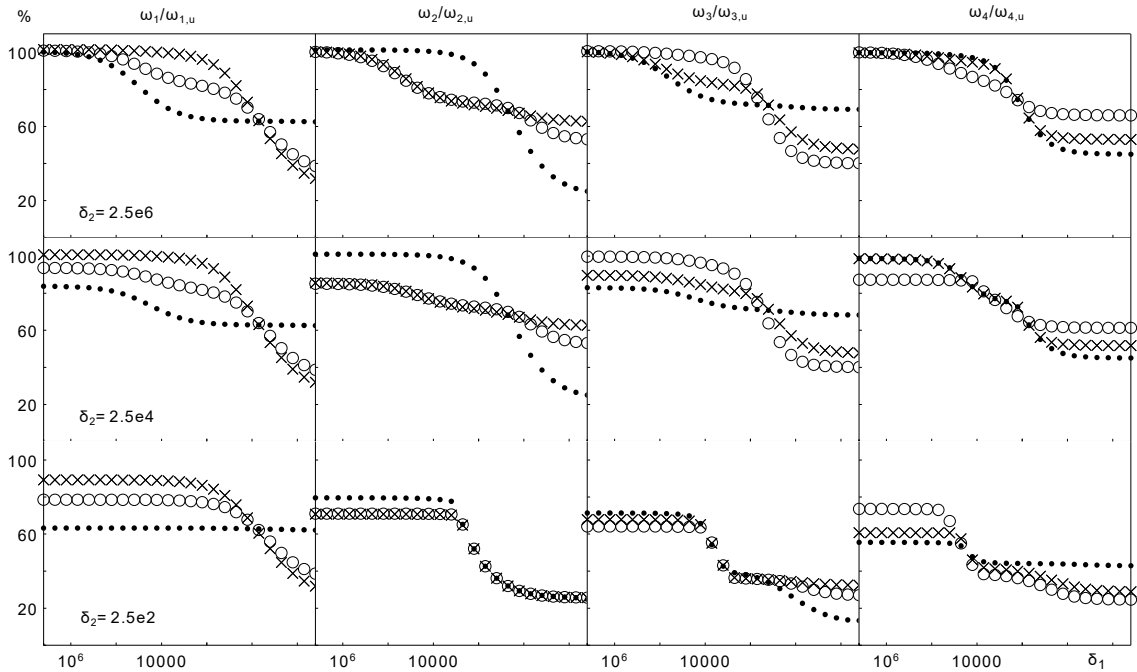


Figure 7: Evolution of the first four natural frequencies ω_i (percentage respect to the frequencies of the undamaged beam, $\omega_{i,u}$), for $\lambda = 1$ (solid), $\lambda = 2$ (circles) and $\lambda = 3$ (cross), with the variation of δ_1 and three fixed values of δ_2 . A value of $\delta_2 = 250$, $\delta_2 = 10$ and $\delta_2 = 0.001$ represents, respectively, a rigid, a damaged and a broken bond.

Now, the parameters to modify are the nondimensional inertia properties s and r_θ , the position of the welded section λ , the nondimensional translational rigidities δ_1 and δ_2 , and the nondimensional torsional rigidities δ_{T1} and δ_{T2} of the left and right-side springs, respectively. Note that, each side of the welding is affected by both translational and torsional rigidities and it has no physical sense to consider the isolated effect of one of them. Therefore, the study will be focused on damage either the right or the left-side on the welding bond via decreasing both rigidities.

In this way, we estimate s, r_θ, δ and δ_T to be

$$s \sim \frac{mL_s}{mL} \sim \frac{L_s}{L}, \quad r_\theta \sim \frac{mL_s(L/\epsilon)^2}{mL^3} \sim \frac{L_s}{\epsilon^2 L}, \quad \delta \sim \frac{EI/L_s^3}{EI/L^3} \sim \left(\frac{L}{L_s}\right)^3 \quad \text{and} \quad \delta_T \sim \frac{EI/L_s}{EI/L} \sim \frac{L}{L_s},$$

where L_s is the welding length, and ϵ the beam slenderness. Again, a welding material similar to the structural one is considered. From this analysis we could also infer the ratio between nondimensional translational and torsional stiffness's of each side given by $\delta / \delta_T \sim 10000$. From now on, the relationship $\delta_i / \delta_{Ti} = 10000$ will be always used. Like for the rod in torsional vibration, we consider a welding length of a 1% of the total length and $\epsilon = 10$ to be consistent with the applicability of the Euler-Bernuilli beam theory.

The mass parameters $s = 0.01$ and $r_\theta = 0.0001$ will be kept constant like in the prior study. The effect of damaging one side of the welding section will be considered first. In Figure 7 the first four natural frequencies are given for different values of the right-side stiffness's with the variation of the left-side rigidities.

In this figure it can be observed the following: for the case of $\lambda = 1$, in contrast with the case of torsional vibration, now all the frequencies, odd and even, are reduced when decreasing rigidity and the reduction can be quite large (closer to 80% for the second frequency when rigidity is low). These results were also observed for a similar model but without lumped mass by Loya et al (2006) and Priyadarshini (2013). Also, for the same frequencies (see $\omega_3 / \omega_{3,u}$) there are two transitions as function of the rigidity, one when the rigidity decrease to a value of 10^4 and a second one when the reduction is closer to a value of 10^2 . The evolution of the frequency in this case can serve as a measure of the grade of the structure.

Now for the bending vibration case, it seems that the influence of the location of welding, values of $\lambda = 1, 2, 3$ in Figure 7, seems to be not as important as in the torsion case since now, for all the locations and frequencies, there is a reduction in frequency when rigidity is decreased.

From this figure, similar conclusions to the rod structural element could be drawn. Defining a new nondimensional frequency parameter $\nu = \omega \sqrt{(mL^3) / (EI)}$, the first four natural frequencies of a double-clamped undamaged beam $\nu_{i,u}$ (where the subscript "i" denotes the i-th mode) are given by 22.37, 61.67, 120.90 and 199.86. In addition, following a similar nomenclature we call $\nu_{i,j}^{s(l)}$ to the i-th frequency of the shorter (larger) cantilevered beam for a value of $\lambda = j$. When the beam is undamaged the frequency parameter coincides with the double-clamped beam natural frequencies in each mode.

Considering the case of $\lambda = 1$ with no welded connection, the frequency parameters for each side of the beam are identical to the cantilevered beam and takes the following values: 14.06, 88.13... given by the analytical solution of the problem. Similarly to the torsional vibrations of the rod, here we also find various frequency changes in some modes. Again, it depends on how many frequencies of the cantilevered beam are smaller than the natural frequency of the undamaged beam. The simplest case is considering a mode with only one frequency below where the system evolves from the undamaged natural frequency to this smaller frequency. In the general case, where several frequencies are below the natural frequency of the mode under consideration, the system evolves from the natural frequency of the undamaged beam to the nearest frequency of the cantilevered system and then, to the next one and so on until no other smaller frequency for the cantilevered beam exists. Then, reducing the stiffness's yields to the vibrations as a lumped mass attached to two springs.

Moreover, one can estimate the threshold where the lumped mass vibrations appears. The translational and rotational frequencies for the lumped mass -written in a dimensionless nomenclature- are given by $\sqrt{(\delta_1 + \delta_2) / s}$ and $\sqrt{(\delta_{T1} + \delta_{T2}) / r_\theta}$, respectively. The ratio could be written as

$$\frac{v_w}{v_{w'}} \sim \sqrt{\frac{\delta_1 + \delta_2}{\delta_{T1} + \delta_{T2}} \frac{r_\theta}{s}} \sim \sqrt{\frac{\delta}{\delta_T} \frac{r_\theta}{s}} \sim \frac{L}{\epsilon L_s}$$

that, for the welding length considered, is 10. Therefore, for a really damaged -practically broken-soldering, the system will vibrate first as a translating lumped mass.

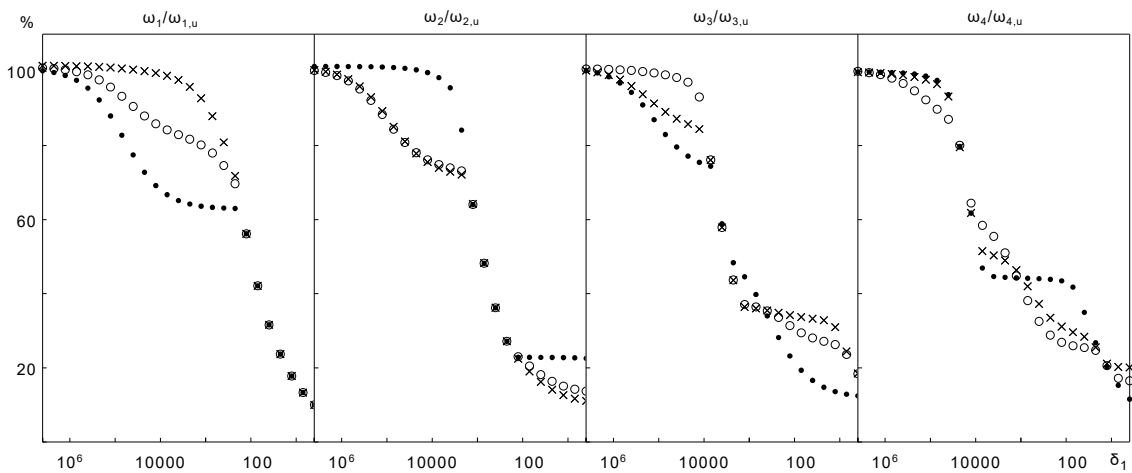


Figure 8: Evolution of the first four natural frequencies ω_i (percentage respect to the frequencies of the undamaged beam, $\omega_{i,u}$), for $\lambda = 1$ (solid), $\lambda = 2$ (circles) and $\lambda = 3$ (cross), with the variation of δ_1

(both springs have the same rigidity, $\delta_1 = \delta_2$, $\delta_{T1} = \delta_{T2}$ and $\delta_{T1} = 10^{-4}\delta_1$).

Now, in Figure 8 the evolution of the first four frequencies of the damaged beam referred to the value of the frequency of the undamaged beam are represented as function of the nondimensional rigidity δ_1 . For this figure it was set $\delta_1 = \delta_2$ and $\delta_{T1} = \delta_{T2}$. Three positions of the welding are considered defined by the values of the parameter $\lambda = 1, 2$ and 3 .

From the figure it is observed that the first frequency is the one that changes more rapidly for $\lambda = 1$ and the second frequency for $\lambda = 2, 3$. With a reduction of rigidity from 10^6 to 10^5 the frequency already changes to a value of 80% for the first frequency (referred to the frequency of the undamaged structure) and $\lambda = 1$; and a similar reduction is observed for the second frequency when $\lambda = 2, 3$. Thus, the method can serve as a good prediction method of damage detection when the reduction of stiffness is still very low.

Finally, the effect of welding inertia is considered. The results are presented in Table 4 and it can be observed again that when the added mass is large (a 2% of the total beam mass) it is no longer possible to recover the dynamic properties of the undamaged beam for all cases (in fact it is only possible for the first frequency, with $\lambda = 2$). The amount of added mass that limit the go back to the

undamaged beam depends on the welded position, thus, for $\lambda = 3$ the fourth frequency cannot be recovered for a value of added mass of 1%. This is a very interesting result for the evaluation of damage of welded structural elements since depending on the added mass, somehow it is needed the starting state of the welded structural element before it can be evaluated if the bond is damaged or not.

λ	s	δ_1 [E6]			
		v_1	v_2	v_3	v_4
2	0.0010	0.2608	0.8425	0.0305	0.5150
	0.0050	0.3275	1.1200	0.0535	0.8235
	0.0100	0.4650	1.8250	0.1460	2.4050
	0.0125	0.5775	2.5425	0.3200	16.375
	0.0150	0.7475	4.1725	2.8750	-
	0.02	1.6980	-	-	-
3	0.0010	0.0069	0.6925	0.7440	0.0830
	0.0050	0.0089	0.9270	1.0325	0.2085
	0.0100	0.1280	1.5245	1.8010	-
	0.0125	0.0157	2.1760	2.7560	-
	0.0150	0.0193	3.6740	5.5495	-
	0.02	0.0305	-	-	-

Table 4: Value of the nondimensional rigidities δ_1 to recover the i-th frequency of the first four natural modes with the variation of the nondimensional welding mass s and r_θ .

$$\text{We take } r_\theta = s / 100 \text{ and } \delta_1 = \delta_2 = 10000\delta_{T1} = 10000\delta_{T2}.$$

4 CONCLUSIONS

A method for the evaluation of the dynamic properties of welded structural elements has been presented. The method can consider any real boundary condition of the element and applications to simpler boundary conditions have been presented.

For the simplest boundary conditions, the analytical approach can be used, leading to a non-linear equation. However, even in these cases, the convergence of numerical methods is arduous. On the other hand, the FEM model can treat different boundary conditions and the eigenvalue method is accurate and fast.

The impact of the welding characteristics in the system response has been presented and discussed. The main conclusion that can be inferred is that soon when rigidity at either side of the welding is decreased the dynamic characteristics of the structural element change enough to be detected. Section 3 presents the most part of the results, where one can see the evolution of the first natural frequencies for different values of the welding stiffness. In fact, this change of the natural frequencies allows to determine the damage of the welding bond. It might be interesting to quantify this damage experimentally to fully validate the proposed method in this work.

The model that we have presented includes the added mass due to the welding process. It has been shown that there exist values of the mass for which the dynamic properties of the undamaged

structural element cannot be recovered. This is a very interesting result since if the method of vibration test is used to detect the damage of a welded element, a reduction of the natural frequencies could already exist from the moment when the element was repaired, due to the added mass. Thus, the dynamic properties of the welded element should be the base to compare with and not the dynamic properties of the undamaged structural element.

Another conclusion that can be drawn from the results presented is that, in general, several frequencies should be considered when evaluating if a welded structural element is damaged. Depending on the welding location the first frequency may not be affected by the loss of rigidity at the bond connection. This result is in contrast to other investigations that used a vibration based method to determine the damage of a beam due to cracks and considered only the change of the first natural frequency.

References

- Abdel-Mooty, M. (2012). Damage Identification in Continuous Structures Using Free Vibration Characteristics. 10th World Congress on Computational Mechanics, July 2012, Sao Paulo, Brazil.
- Adams, R.D., Cawley, P., Pye, C.J. and Stone, B.J. (1978). A vibration technique for non-destructively assessing the integrity of structures. *Journal of Mechanical Engineering Science*. 20:93-100.
- Chondros, T.G. and Labeas, G.N. (2007). Torsional Vibration of a Cracked Rod by Variational Formulation and Numerical Analysis. *Journal of Sound and Vibration* 301:994-1006.
- Chondros, T.G. and Dimarogonas, A.D. (1980). Identification of cracks in welded joints of complex structures. *Journal of Sound and Vibration*. 69:531-538.
- Chondros, T.G., Dimarogonas, A.D. and Yao, J. (1998 a)). A Continuous Cracked Beam Vibration Theory. *Journal of Sound and Vibration*. 215:17-34.
- Chondros, T.G., Dimarogonas, A.D. and Yao, J. (1998 b)). Longitudinal Vibration of a Continuous Cracked Bar. *Engineering Fracture Mechanics*. 61:593-606
- Dimarogonas, A.D. (1996). Vibration of Cracked Structures: A State of the Art Review. *Engineering Fracture Mechanics*. 55:831-857.
- Eslami, G., Maleki, V.A. and Rezaee, M. (2016). Effect of Open Crack on Vibration Behavior of a Fluid-Conveying Pipe Embedded in a Visco-Elastic Medium. *Latin American Journal of Solids and Structures*. 13 (1):136-154.
- Gomaa, F.R., Nasser, A.A. and Ahmed, Sh.O. (2014). Sensitivity of Modal Parameters to Detect Damage through Theoretical and Experimental Correlation. *International Journal of Current Engineering and Technology*. 4:172-181.
- Halmshaw, R. (1987). *Nondestructive Testing*. Edward Arnold.
- Kindova-Petrova, D. (2014). Vibration-Based Methods for Detecting a Crack in a Simply Supported Beam. *Journal of Theoretical and Applied Mechanics*, 44:69-82.
- Kisa, M. and Brandon, J. (2000). The Effects of Closure of Cracks on the Dynamics of a Cracked Cantilever Beam. *Journal of Sound and Vibration*. 238:1-18.
- Loya, J.A., Rubio, L. and Fernandez-Saez, J., (2006). Natural frequencies for bending vibrations of Timoshenko cracked beams. *Journal of Sound and Vibration* 290:640-653.
- Morassi, A. (2001). Identification of a Crack in a Rod Based on Changes in a Pair of Natural Frequencies. *Journal of Sound and Vibration*. 242:577-596.
- Mostafa, M. and Tawfik, M. (2016) Crack Detection Using Mixed Axial and Bending Natural Frequencies in Metallic Euler-Bernuilli Beam. *Latin American Journal of Solids and Structures*. 13(9):1641-1657.
- Petyt, M. (1990). *Introduction to Finite Element Vibration Analysis*. Great Britain: Cambridge University Press.

- Priyadarshini, A. (2013). Identification of Cracks in Beams Using Vibration Analysis. Master Science Thesis. Department of Civil Engineering. National Institute of Technology, Rourkela, India.
- Rizos, P.F. and Aspragathos, N. (1990). Identification of Crack Location and Magnitude in a Cantilever Beam from the Vibration Modes. *Journal of Sound and Vibration*. 138:381-388.
- Saavedra, P., Baquedano, D. and San Juan, L. (1996). Modelo Numérico para el Estudio Dinámico de un Rotor con Eje Agrietado. *Revista Internacional de Métodos Numéricos para Cálculo y Diseño en Ingeniería*. 12:125-146.
- Shang, D., Barkey, M.E., Wang, Y. and Lim, T.C., (2003). Effect of Fatigue Damage on the Dynamic Response Frequency of Spot-Welded Joints. *International Journal of Fatigue*. 25:311-316
- Smart, M. and Chandler, H.D. (1995). Modal testing for NDT of structures. *R and D Journal*. 11:79-85.
- Sohn, H., Farrar, C.H., Fugate, M.L. and Czarnecki, J.J. (2001). Structural Health Monitoring of Welded Connections. The First International Conference on Steel and Composite Structures, Pusan, Korea, June 14-16.
- Yunus, M.A., Rani, M.N., Ouyang, H., Deng, H. and James, S. (2011). Identification of Damaged Spot Welds in a Complicated Joined Structure. *Journal of Physics*, 305, DOI:10.1088/1742-6596/305/1/012057.